

Making a splash on an incline

Jean-Luc Thiffeault

Department of Mathematics
University of Wisconsin – Madison

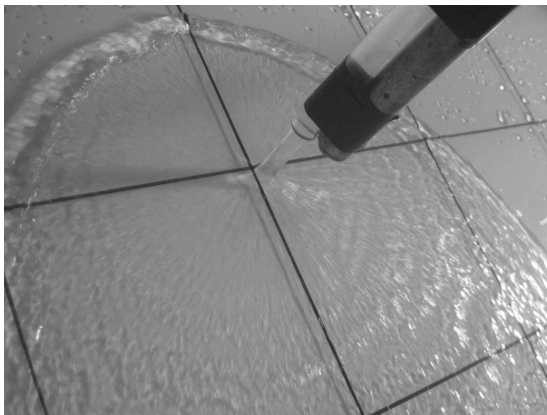
with Andrew Belmonte (Penn State), Khalid Kamhawi, and Jay Johnson (UW)

Joe Keller's 90th birthday
Stanford University, 26 October 2013

Supported by NSF grants DMS-1109315 and CMMI-1233935



A jet hitting an inclined plane



Plane inclined at 45° . The flow rate is $Q \simeq 120 \text{ cm}^3 \text{ s}^{-1}$.

[with Andrew Belmonte in Claudia Cenedese and Karl Helfrich's lab at Woods Hole, GFD 2008]

Try steady potential flow: $\mathbf{u} = \nabla\varphi$, with

$$\begin{aligned}\nabla^2\varphi &= 0, && \text{mass conservation;} \\ \frac{1}{2} |\nabla\varphi|^2 + \frac{p}{\rho} - \mathbf{g} \cdot \mathbf{r} &= H, && \text{Bernoulli's law;}\end{aligned}$$

Boundary conditions:

$$\begin{aligned}\partial_z\varphi &= 0 && \text{at } z = 0, && \text{no-throughflow at substrate;} \\ \nabla\varphi \cdot \nabla h &= \partial_z\varphi && \text{at } z = h, && \text{kinematic condition at free surface;} \\ p &= 0 && \text{at } z = h, && \text{constant pressure at free surface.}\end{aligned}$$

Here z is normal to the substrate, x_1 and x_2 are parallel to it.

Expand Bernoulli's law in the small fluid depth ε :

$$\sum_{j=1}^2 (\partial_j \varphi)^2 + \varepsilon^{-2} (\partial_z \varphi)^2 + \frac{2p}{\rho} - 2\mathbf{g} \cdot (\mathbf{X} + \varepsilon z \hat{\mathbf{e}}_3) = 2H,$$

where $\mathbf{X} = x_1 \hat{\mathbf{e}}_1 + x_2 \hat{\mathbf{e}}_2$. Also expand φ :

$$\varphi(x_1, x_2, z) = \varphi_{(0)} + \varepsilon \varphi_{(1)} + \varepsilon^2 \varphi_{(2)} + \dots,$$

to obtain at leading order $\partial_z \varphi_{(0)} = 0$, so that

$$\varphi_{(0)} = \Phi(x_1, x_2).$$

At next order:

$$\sum_{j=1}^2 (\partial_j \Phi)^2 + (\partial_z \varphi_{(1)})^2 + \frac{2p}{\rho} - 2\mathbf{g} \cdot \mathbf{X} = 2H,$$

Evaluate at $z = h$ and use the boundary conditions:

$$\sum_{j=1}^2 (\partial_j \Phi)^2 - 2\mathbf{g} \cdot \mathbf{X} = 2H,$$

Differentiate to get rid of constant:

$$\sum_{j=1}^2 \partial_j \Phi \partial_{ij} \Phi = \mathbf{g} \cdot \partial_i \mathbf{X}, \quad i = 1, 2.$$

Introduce the characteristics $x_1(\tau)$, $x_2(\tau)$:

$$\dot{x}_1 = \partial_1 \Phi(\mathbf{x}), \quad \dot{x}_2 = \partial_2 \Phi(\mathbf{x}),$$

We have $\partial_{ij} \Phi = \partial_i \dot{x}_j$ and $\ddot{x}_i = (\partial_j \dot{x}_i) \dot{x}_j = \partial_j \Phi \partial_{ij} \Phi$, so that

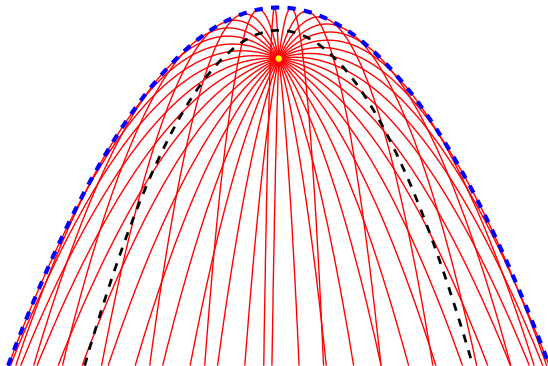
$$\ddot{x}_i = \mathbf{g} \cdot \hat{\mathbf{e}}_i, \quad i = 1, 2.$$

[Rienstra (1996)]

Characteristics for a jet striking an inclined plane



The characteristics have a parabolic envelope (blue dashed):



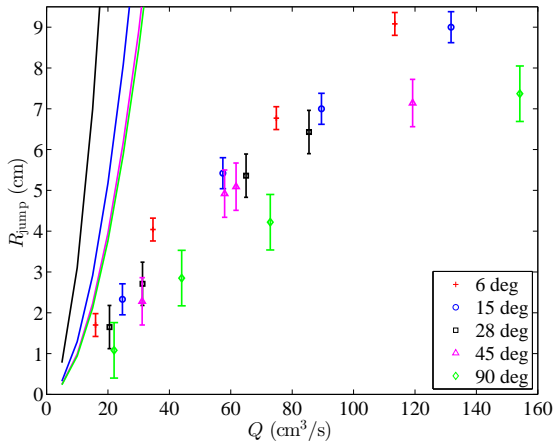
Edwards *et al.* (2008) used the 'delta-shock' framework to account for characteristics crossing: this lowers the rise distance by $5/9$, and the profile remains essentially parabolic (black dashes).

Comparison with experiments



Compare ballistic rise distance $U^2/2g \sin \theta$ to experiments:

[Thiffeault & Belmonte (2010)]



Not so good... even if we lower the curves by 5/9 following Edwards *et al.* (2008).



- [Watson \(1964\)](#): inviscid and viscid, but assumes position of jump.
- Many subsequent refinements: [Bohr *et al.* \(1993\)](#); [Godwin \(1993\)](#); [Bohr *et al.* \(1997\)](#); [Brechet & Néda \(1999\)](#); [Chang *et al.* \(2001\)](#); [Bush & Aristoff \(2003\)](#). . . .
- Jet striking a horizontal plate at an oblique angle: [Sparrow & Lovell \(1980\)](#); [Rubel \(1981\)](#); [Kate *et al.* \(2007\)](#).
- Jet striking a moving plate: [Gradeck *et al.* \(2006\)](#); [Kate *et al.* \(2009\)](#).
- Microdecorated surface: [Dressaire *et al.* \(2009\)](#).
- Many contributions on jets by Joe: [Keller *et al.* \(1973\)](#); [Keller & Geer \(1973\)](#); [Vanden-Broeck & Keller \(1982\)](#); [Ting & Keller \(1990\)](#). . . .
- Here we'll adapt the model of [Bohr *et al.* \(1993\)](#) to an inclined plane. Our main assumption is that, as far as the rise distance is concerned, the jet is 'locally' circular.



Let's cheat and assume that the jet is hitting an inverted cone, so that the system is axially-symmetric.

Following Bohr *et al.* (1993), start with boundary layer equations:

$$u \frac{\partial u}{\partial r} + w \frac{\partial u}{\partial z} = -g \cos \theta \frac{dh}{dr} - g \sin \theta + \nu \frac{\partial^2 u}{\partial z^2}$$
$$\frac{\partial u}{\partial r} + \frac{u}{r} + \frac{\partial w}{\partial z} = 0$$

where $u(r, z)$ and $w(r, z)$ are respectively the velocity components tangent and perpendicular to the solid surface.

r is tangent to the solid surface, and z is perpendicular to it.

A simple model with viscosity II



The boundary conditions at the bottom and top of the fluid are

$$\begin{aligned} u = 0, \quad w = 0, \quad & \text{at } z = 0; \\ \frac{\partial u}{\partial z} = 0, \quad w = u \frac{dh}{dr}, \quad & \text{at } z = h(r). \end{aligned}$$

Integrating gives the mass conservation equation

$$r \int_0^h u(r, z) dz = q$$

where $q = Q/2\pi$, with Q the flow rate of the jet.

In addition, we must specify the velocity $u(r_0, z) = u_0(z)$ and height $h(r_0) = h_0$ at a radius r_0 larger than the jet radius, since the boundary layer equations are not valid directly under the jet.

We use the standard hydraulic jump scalings to define dimensionless 'tilde' variables:

$$\begin{aligned}u &= \alpha \tilde{u}, & \alpha &= (c_1^{-1/2} c_2^{1/8}) q^{1/8} \nu^{1/8} (g \cos \theta)^{3/8}, \\w &= \beta \tilde{w}, & \beta &= q^{-1/4} \nu^{3/4} (g \cos \theta)^{1/4}, \\r &= \Gamma \tilde{r}, & \Gamma &= (c_1^{1/2} c_2^{-3/8}) q^{5/8} \nu^{-3/8} (g \cos \theta)^{-1/8}, \\z &= \delta \tilde{z}, & \delta &= (c_2^{1/4}) q^{1/4} \nu^{1/4} (g \cos \theta)^{-1/4},\end{aligned}$$

except that we included the $\cos \theta$ dependence in the scalings.

We immediately drop the tildes.

(We will discuss the dimensionless constants c_1 and c_2 below.)

Upon averaging in the z direction, the boundary-layer equation becomes after integration by parts

$$2\overline{u} \frac{\partial \overline{u}}{\partial r} + \frac{1}{r} \overline{u^2} + \frac{h'}{h} \overline{u^2} \Big|_{z=h} = -c_1 \left(G + \frac{dh}{dr} \right) - \frac{c_1}{c_2} \frac{1}{h} \frac{\partial u}{\partial z} \Big|_{z=0}$$

where the z -average of a function $F(r, z)$ is

$$\overline{F}(r) = (1/h) \int_0^h F(r, z) dz$$

and we defined

$$G = (c_1^{1/2} c_2^{-5/8}) q^{3/8} \nu^{-5/8} (g \cos \theta)^{1/8} \tan \theta.$$

We now assume the separable form

$$u(r, z) = v(r)f'(z/h(r)),$$

where $v = \bar{u}$ is the averaged profile, f is a given function that describes the vertical structure of the thin layer, with $f(0) = f'(0) = f''(1) = 0$, $f(1) = 1$.

Mass conservation integral becomes simply $vh = 1$, which gives a relationship between v and h . This allows us to derive the two relations

$$2\overline{u\frac{\partial u}{\partial r}} + \frac{1}{r}\overline{u^2} + \frac{h'}{h}u^2|_{z=h} = c_1 v \frac{\partial v}{\partial r}, \quad \left. \frac{\partial u}{\partial z} \right|_{z=0} = c_2 \frac{v}{h},$$

with

$$c_1 = \int_0^1 f'^2(\eta) d\eta \quad \text{and} \quad c_2 = f''(0).$$



The two relations can be used in the earlier averaged equations to obtain

$$vv' + h' = -\frac{v}{h^2} - G, \quad vhr = 1.$$

For $G = 0$ these reduce to the equations of Bohr *et al.* (1993), which are essentially as derived by Kurihara (1946) and Tani (1949).

Combine into one ODE for $v(r)$:

$$r(1 - rv^3)v' = -(1 - Gr^2v - r^4v^4)v,$$

which must be solved together with the flux boundary condition $v(r_0) = v_0$ at the jet radius r_0 .



$$r(1 - rv^3)v' = -(1 - Gr^2v - r^4v^4)v$$

Singularity at $rv^3 = 1$ will determine the location of the hydraulic jump ($v' \rightarrow -\infty$), which we will associate here with the rise distance.

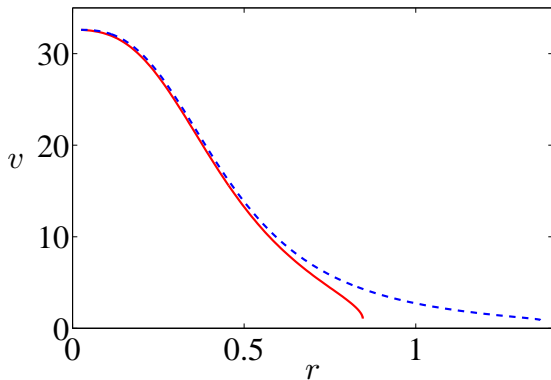
Since $G = G(Q, \theta)$, this ODE will have to be solved at each inclination angle and flow rate.

When doing numerical calculations, use the parabolic profile

$$f(\eta) = \frac{3}{2}\eta^2 - \eta^3,$$

from which $c_1 = 6/5$, $c_2 = 3$. A more general approach, using a variable cubic profile as in Bohr *et al.* (1997), doesn't much change the scaling.

For $Q \simeq 119 \text{ cm}^3 \text{ s}^{-1}$ and $\theta = 45^\circ$:



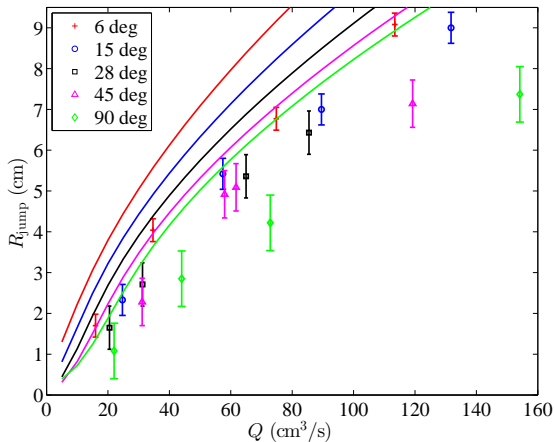
Solid red: $G = 67$; **blue dashed:** $G = 0$.

(Fairly insensitive to jet radius r_0 .)

Comparison to experiments

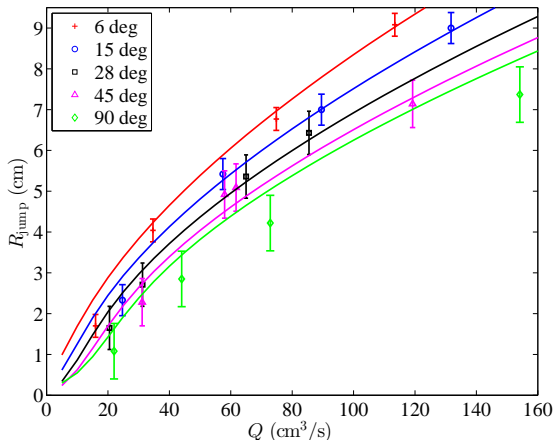


This overestimates the rise height, unsurprisingly:



But the scaling looks pretty good...

Let's cheat and multiply by fitted parameter **0.76**, to adjust for the singularity position occurring beyond the actual jump:



Not so bad... , except at **90°** (vertical wall). [Thiffeault & Belmonte (2010)]

Rienstra (1996) also applied his inviscid model to curved surfaces (spheres, cylinders). Here's my attempt at an experiment [Thiffeault & Kamhawi (2008)]:



Compare to characteristics on a cylinder:



Rienstra (1996) treated surfaces with global orthogonal coordinates (plane, cylinder, sphere).

What about more general surfaces?

Write x^1, x^2 for general 2D coordinates that locate a point on the substrate. A small-thickness expansion similar to Rienstra's yields for the characteristics [Thiffeault & Kamhawi (2008)]:

$$\ddot{x}^\sigma + \Gamma_{\alpha\beta}^\sigma \dot{x}^\alpha \dot{x}^\beta = \mathbf{g} \cdot \mathbf{e}^\sigma$$

where $\Gamma_{\alpha\beta}^\sigma$ are the **Christoffel symbols** for the shape of the substrate.

This is the **geodesic equation** with a gravitational forcing. The fluid particles (characteristics) are trying to follow straight lines, but their trajectories are bent by the substrate curvature and gravity.

The geodesic equations are actually a **fourth-order** autonomous system.

Hence, chaos is a possibility, **as long as the substrate does not possess a continuous symmetry!** (Ruled out for plane, cylinder, sphere.)

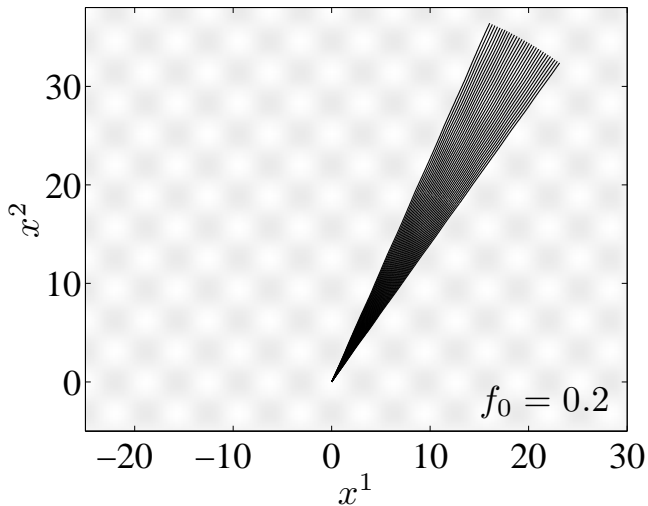
Consider a simple substrate shape parametrized by:

$$f(x^1, x^2) = f_0 \cos x^1 \cos x^2$$

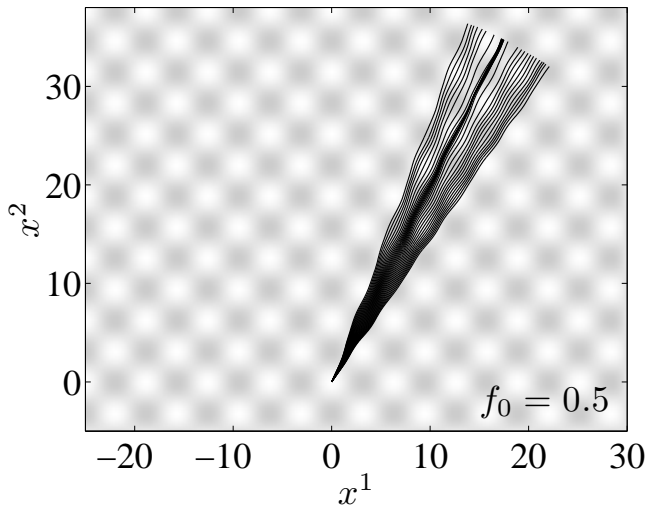
Horizontal substrate: $f_0 = 0.2$



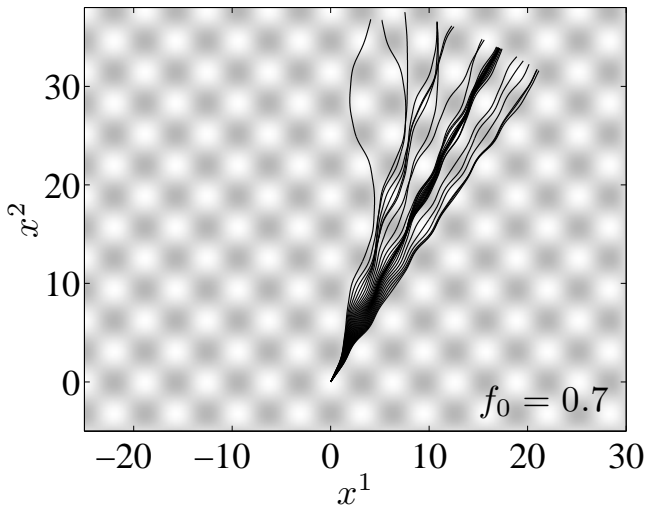
First take $g = 0$ and keep the surface horizontal.



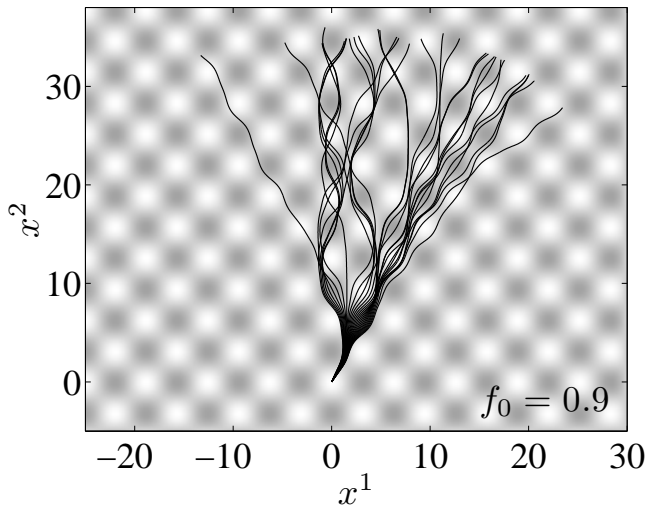
Horizontal substrate: $f_0 = 0.5$



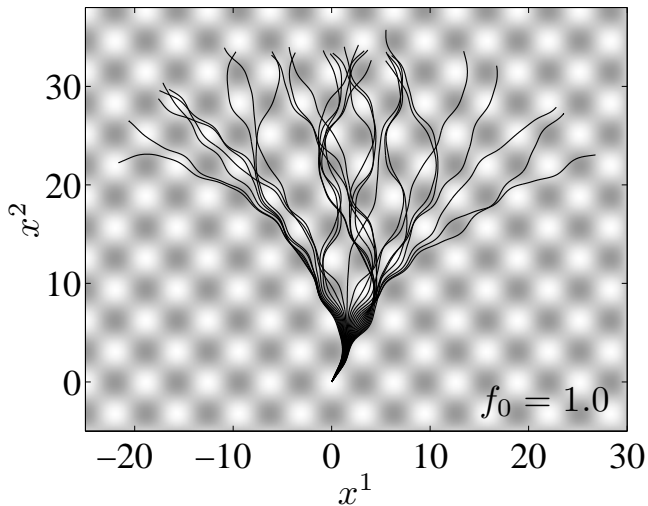
Horizontal substrate: $f_0 = 0.7$



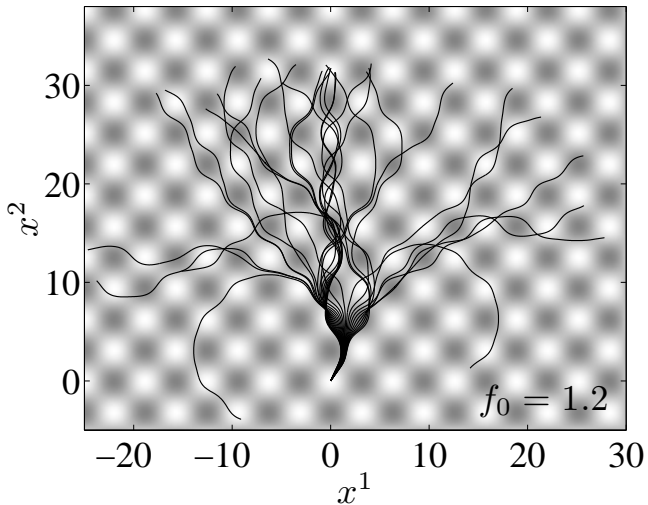
Horizontal substrate: $f_0 = 0.9$



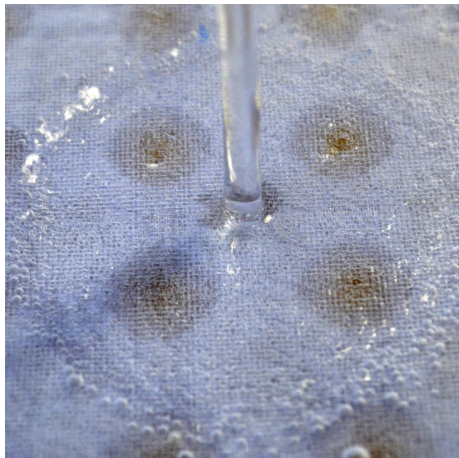
Horizontal substrate: $f_0 = 1.0$



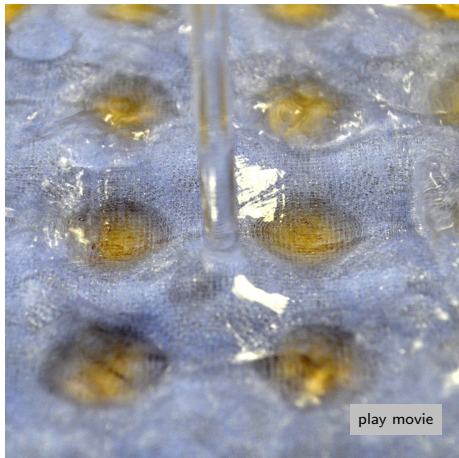
Horizontal substrate: $f_0 = 1.2$



Experiments with 3D-printed substrate



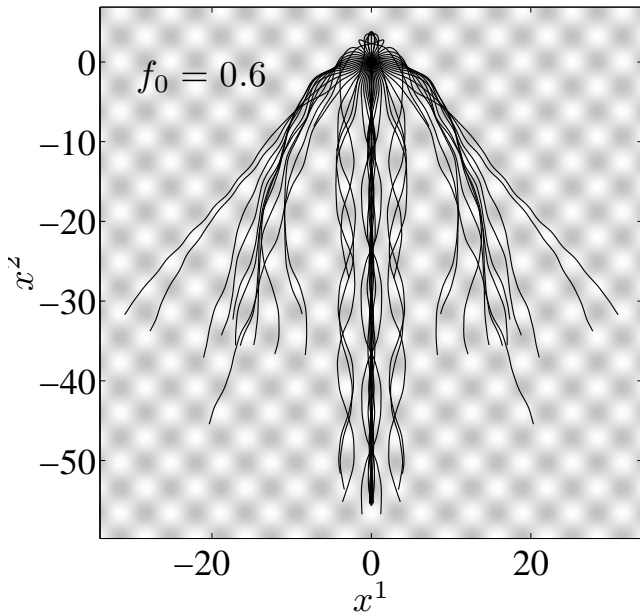
Flat substrate

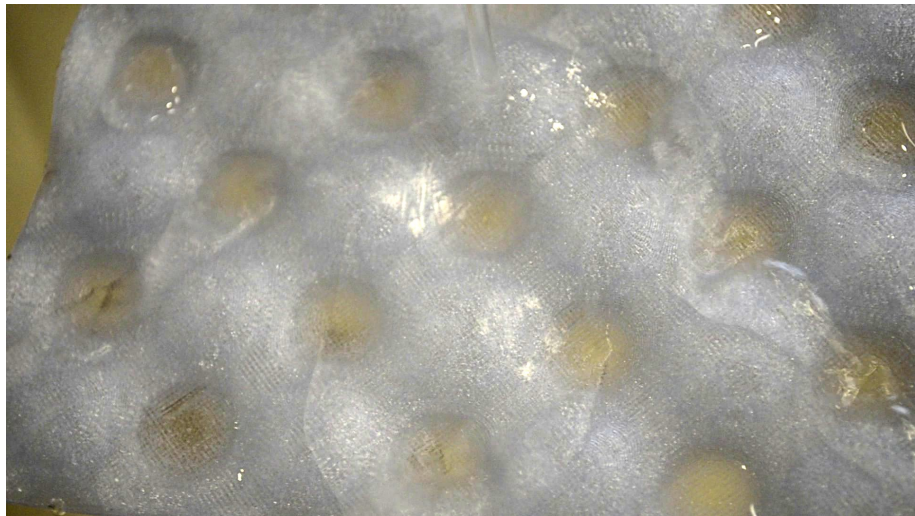


Patterned substrate

Jump is about 50% larger for a flat substrate. [Experiments with Jay Johnson.]

Inclined substrate: $f_0 = 0.6$





The simple model correctly predicts the multiple 'paths'.

[Experiment with Jay Johnson.]



- Bohr, T., Dimon, P., & Putkaradze, V. (1993). *J. Fluid Mech.* **254**, 635–648.
- Bohr, T., Putkaradze, V., & Watanabe, S. (1997). *Phys. Rev. Lett.* **79** (6), 1038–1041.
- Brechet, Y. & Néda, Z. (1999). *Am. J. Phys.* **67** (8), 723–731.
- Bush, J. W. M. & Aristoff, J. M. (2003). *J. Fluid Mech.* **489**, 229–238.
- Chang, H.-C., Demekhin, E. A., & Takhistov, P. V. (2001). *Journal of Colloid and Interface Science*, **233**, 329–338.
- Dressaire, E., Courbin, L., Crest, J., & Stone, H. A. (2009). *Phys. Rev. Lett.* **102** (19), 194503.
- Edwards, C. M., Howison, S. D., Ockendon, H., & Ockendon, J. R. (2008). *IMA J. Appl. Math.* **73** (1), 137–157.
- Godwin, R. P. (1993). *Am. J. Phys.* **61** (8), 829–832.
- Gradeck, M., Kouachi, A., Dani, A., Amoult, D., & Boréan, J. L. (2006). *Exp. Therm. Fluid Sci.* **30**, 193–201.
- Kate, R. P., Das, P. K., & Chakraborty, S. (2007). *J. Fluid Mech.* **573**, 247–263.
- Kate, R. P., Das, P. K., & Chakraborty, S. (2009). *J. Fluids Eng.* **131** (3), 034502.
- Keller, J. B. & Geer, J. (1973). *J. Fluid Mech.* .
- Keller, J. B., Rubinow, S. I., & Yu, Y. O. (1973). *Phys. Fluids*, **16** (12), 2052.
- Kurihara, M. (1946). *Rep. Research Institute for Fluid Engineering (Kyusyu Imperial University, "Ryutai Kougaku Kenkyusho Kiyou")*, **3**, 11–33. in Japanese.



- Rienstra, S. W. (1996). *Z. Angew. Math. Mech.* **76** (S5), 423–424.
- Rubel, A. (1981). *AIAA J.* **19**, 863–871.
- Sparrow, E. M. & Lovell, B. J. (1980). *ASME, Ser. C: J. Heat Transfer*, **102**, 202–209.
- Tani, I. (1949). *J. Phys. Soc. Japan*, **4**, 212–215.
- Thiffeault, J.-L. & Belmonte, A. (2010). arXiv:1009.0083.
- Thiffeault, J.-L. & Kamhawi, K. (2008). In: *Chaos, Complexity, and Transport: Theory and Applications*, (Chandre, C., Leoncini, X., & Zaslavsky, G., eds) pp. 40–54, Singapore: World Scientific.
- Ting, L. & Keller, J. B. (1990). *SIAM J. Appl. Math.* **50** (6), 1533–1546.
- Vanden-Broeck, J. M. & Keller, J. B. (1982). *J. Fluid Mech.* **124**, 335–345.
- Watson, E. J. (1964). *J. Fluid Mech.* **20** (3), 481–499.